Rare B_s and B^0 decays at $D\emptyset$

(list people who are involved)

1 Introduction

The subject of rare B-meson decays can be classified in analogy to the K-meson system, into those exhibiting either direct or indirect CP violation, those inolving a flavor changing neutral current, or that explicitly access one of the CKM matrix elements.

In what follows we examine a number of decay modes in the B_s system that are accessible with the $D\emptyset$detector using the current BANA/AAtrack analysis formats. For each of the decays we examine the current state of the decay in terms of its observed branching fraction or the current limits on the the observation of the decay. We also discuss the decay topology and the final state signature for the decay as well as appropriate normalizations.

The decays discussed herein are roughly grouped by the physics of interest that they access, and when available the limits on fundamental properties (i.e. mass of effective propagators for new physics) and compared to their equivalent decays in other systems.

2 Flavor Changing Neutral Currents (FCNC)

One of the strengths of the B sector is its ability to access a number of different flavor changing neutral current processes. The types of currents can be divided based on the total change in quark flavor where we recognize that the B_s system can exhibit both $\Delta B = 1$ and as well as $\Delta s = 1$ currents.

2.1 Leptonic $\Delta B = 1,\ \Delta S = 1$ decays

The dileptonic final state decays of the B_s all exhibit both the $\Delta B = 1$ and $\Delta S = 1$ FCNCs. Each of the decays proceeds through the standard set of box and penguin diagrams as shown in Figure 1 and **??**. The diagrams are effectively equivalent in terms of physics reach, where the actual amplitudes are proportional to the final state lepton masses and the quark couplings. To date none of the decays modes have been observed in the B_s or B^0 sector.

2.1.1 $B_s \to \mu^+\mu^-$

The $B_s \to \mu^+\mu^-$ channel is directly analogous to the observed decay $K_L^0 \to \mu^+\mu^-$. In the B system the dominant couplings though shifts from being to the CKM elements and V_{td} and Vts are instead by the B couplings such that the amplitude becomes proportional to $V_{tb}V_{ts}^*$. When we look at this in terms of the CKM matrix

$$\begin{pmatrix} d' \\ s' \\ b' \end{pmatrix} = \begin{pmatrix} V_{ud} & V_{us} & V_{ub} \\ V_{cd} & V_{cs} & V_{cb} \\ V_{td} & V_{ts} & V_{tb} \end{pmatrix} \begin{pmatrix} d \\ s \\ b \end{pmatrix} \tag{1}$$

It becomes clear that in the Wolfenstien parametrization the B_s decay decouples the dependence of the amplitude on the Wolfenstien ρ and η.

$$\mathbf{V} = \begin{pmatrix} 1 - \frac{1}{2}\lambda^2 & \lambda & A\lambda^3(\rho - \imath\eta) \\ -\lambda & 1 - \frac{1}{2}\lambda^2 & A\lambda^2 \\ A\lambda^3(1 - \rho - \imath\eta) & -A\lambda^2 & 1 \end{pmatrix} \tag{2}$$

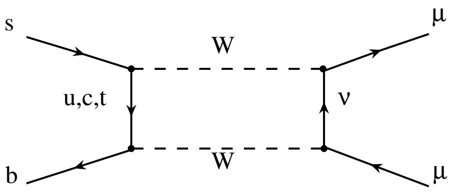

(a) Box diagram for $B_s \to \mu^+\mu^-$

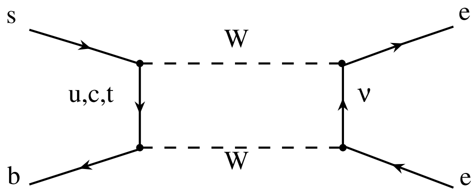

(b) Box diagram for $B_s \to e^+e^-$

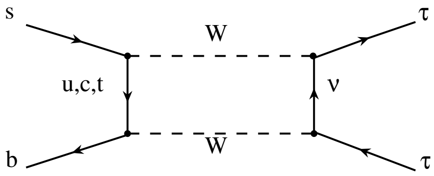

(c) Box diagram for $B_s \to \tau^+\tau^-$

Figure 1: Dileptonic FCNC box diagrams for the B_s system.

In this case the amplitude for $B_s \to \mu^+\mu^-$ gives us:

$$Re(V_{ts}^* V_{tb}) = -A\lambda^2 \tag{3}$$

Which gives us a direct measure of the the Wolfenstien parameter A.

For this reason alone the $\mu^+\mu^-$ amplitude is important to our understanding of the unitarity of the CKM matrix.

In the case of $B_s \to \mu^+\mu^-$ the current limit on the observation of the decay is currently reported at 4.7×10^{-8}, compared to the observed $K_L^0 \to \mu^+\mu^-$ rate of 6.84×10^{-9}. This means the observation of $B_s \to \mu^+\mu^-$ is well within the sensitivity of the $D\emptyset$data sets, as a prediction of the branching fraction can be made based upon the difference in the $t \to b$ and $t \to d$ rates.

The final state topology for the $B_s \to \mu^+\mu^-$ channel is a trivial, displaced two body vertex reconstruction, where backgrounds are suppressed through a co-linearity or "pt_{rel}" requirement between the daughters and the B_s flight path defined by the impact point and the reconstructed vertex.

2.1.2 $B_s \to e^+e^-$

The decay $B_s \to e^+e^-$ is similar in many respects to the $\mu^+\mu^-$ channel with the exception that the decay rate is helicity suppressed by the final state electrons. The interest in the decay comes from the deviation of the rate from the fully suppressed prediction in analog to the $K_L^0 \to e^+e^-$, where the experimentally observed rate is in excess of the fully suppressed prediction. Verification a similar excess in the B sector would be indications for an extra channel for the coupling to the dielectron final state which did not have the same restrictions, as the amplitude coupled through the W^+ to the left-handed q or $\bar{q}$.

The current limit on the observation of $B_s \to e^+e^-$ is only 5.4×10^{-5}, and while the kaon sector would indicate that a fully suppressed channel would have branching fraction approaching $10^{-10} - 10^{-11}$ (based on the observed $9x10^{-12}$ kaon rate) a large unexpected change to the helicity suppression could bring this decay into the observable range for a the full $D\emptyset$data set.

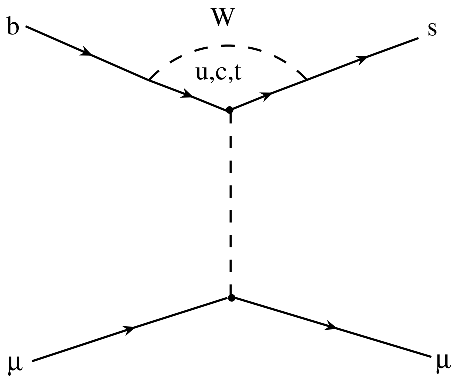

(a) Penguin diagram for $B_s \to \mu^+\mu^-$

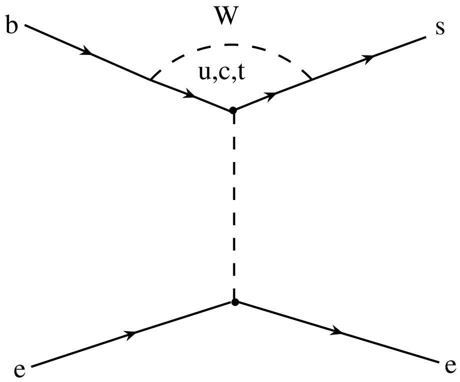

(b) Penguin diagram for $B_s \to e^+e^-$

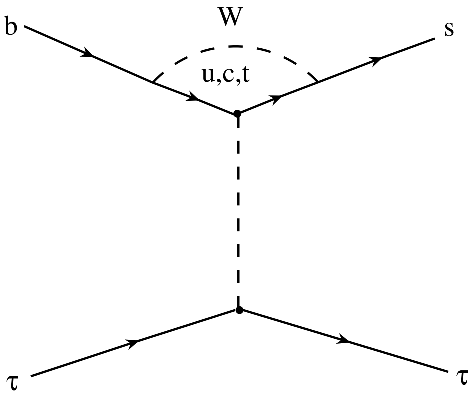

(c) Penguin diagram for $B_s \to \tau^+\tau^-$

Figure 2: Dileptonic FCNC penguin diagrams for the B_s system.

Decay	Limit	Source
$B_s \to \mu^+\mu^-$	4.7×10^{-8}	CDF PRL 100 101802
$B_s \to e^+e^-$	5.4×10^{-5}	L3 PL B391 481
$B_s \to \tau^+\tau^-$	None	None

Table 1: Limits on Dilepton B_s decays.

2.1.3 $B_s \to \tau^+\tau^-$

The dilepton mode that takes the B_s into a τ pair has the same physics sensitivities in terms of its access to the CKM matrix, but had the advantage of having a much larger final state lepton mass which increases the expected branching fraction.

The difficulty with detecting the mode is tagging the two τ's and obtain the energy/momentum measure on each to reconstruct the invariant B_s mass with enough resolution to both separate it from a general E&M combinatorial background, and resolve the vertexing enough to provide a measure of pt_{rel} for the decay to form a tight signal box.

There is currently no limit available for the decay $B_s \to \tau^+\tau^-$.

2.1.4 Multi Letpon FCNC auxiarly measurements

While the dilepton decay modes offer a method of measuring the couplings of the CKM matrix, the actual connection between the experimentally observed decay rate and the actual amplitude of interest which can be connected to the Wolfenstien parameters.

Primarily the problem is disentangling the the short distance W/Z mediated amplitudes represented in the box and penguin diagrams of figure 3, with the long distance amplitudes represented by the class of diagrams where the final state leptons are coupled to a photonic intermediate state as in figure 4.

The measurement of the long distance amplitude is found through measuring the four lepton final state decays in the form of $B_s \to \mu^+\mu^-e^+e^-$, $B_s \to \mu^+\mu^-\mu^+\mu^-$, and $B_s \to e^+e^-e^+e^-$ and there by subtracting off the common $\gamma^*\gamma^*$vertex diagrams which constitute the long distance, or absorptive amplitudes.

Of the four lepton final states, the most important to measure is the $\mu^+\mu^-e^+e^-$final state owing to it's total distinct final state. This removed the interference diagrams that come from final state particle interchange, and directly accesses the diagrams we want.

The event topology is similar to that of many other dimuon final state decays, and detection would be similar to a $B_s \to J/\Psi\phi$ final state, where the kaons coming from the ϕ are replaced with a di-EM signature for the electron pair. More over the expected branching fraction for each of the decays can be down to be considerably greater than the corresponding di-lepton final state, due to the nature of the contributing diagrams and the lack of helicity suppression in the final state. This make the four lepton decay modes of the B_s prime candidates for observation in any program that aims at accessing the dilepton modes.

2.2 Associated $\Delta B = 1$ decays

The second class of FCNC decays that are of interest in the B_s system are the class of decay modes that feature a di-lepton final state, paired with an associated meson. The most interesting of these decays are those that arise through a weak penguin configuration, where a $b \to s$ or $b \to d$ transition can occur on one of the quark lines.

2.2.1 $B_s \to K^0_S\mu^+\mu^-$

The decay mode $B_s \to K^0_S\mu^+\mu^-$ is an associated decay that directly accesses the $b \to d$ penguin diagrams of figure 5.

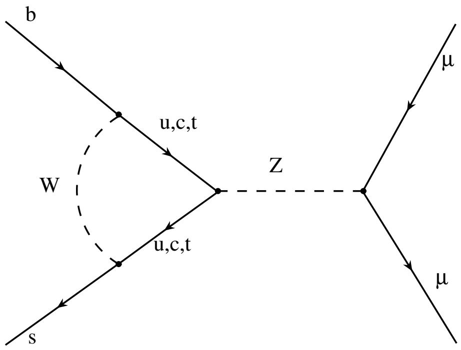

(a) Short distance penguin 1

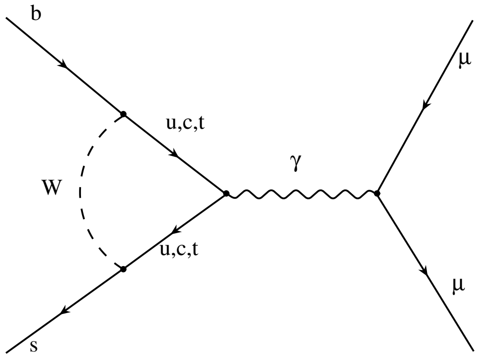

(b) Short distance penguin 2

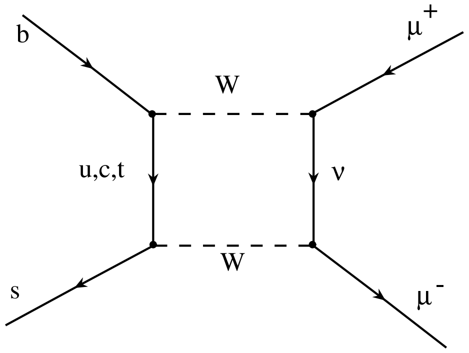

(c) Short distance box

Figure 3: Short distance contributions to the $B_s \to \mu^+\mu^-$ amplitude.

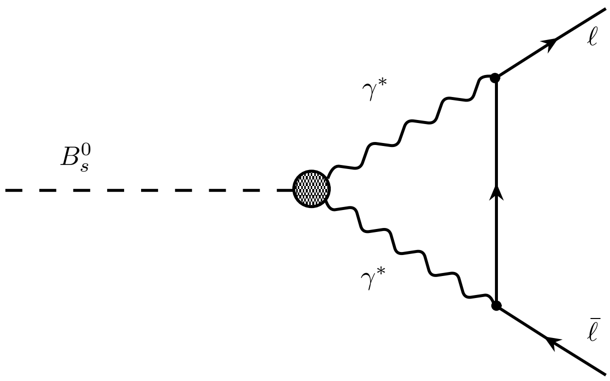

Figure 4: Leading order absorptive contribution to $B_s \to \ell\bar{\ell}$ via a real two photon intermediate state

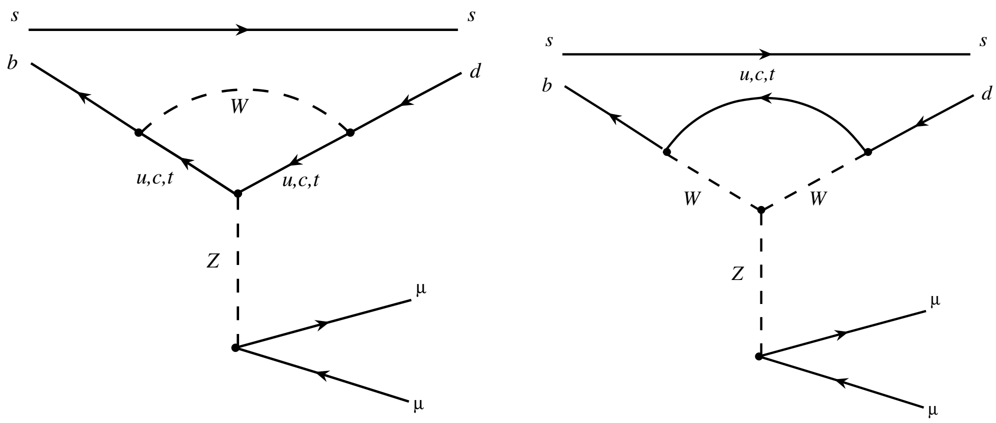

(a) $B_s \to K^0_S \mu^+\mu^-$ penguin 1

(b) $B_s \to K^0_S \mu^+\mu^-$ penguin 2

Figure 5: Associated decay $B_s \to K^0_S \mu^+\mu^-$.

The value of measuring the amplitude is not only in the almost direct measurement it provides of of $V^*_{tb}V_{td}$; because of the value of V_{tb} approaches unity, this then equates to an almost direct measure the Wolfenstien ρ and η, though the real and imaginary parts of the amplitude. Yet the three body semileptonic decays can also be parameterized in terms of the the helicity angles defined the associated meson and the lepton pair. Since the lepton pair does not come from an on-shell particle, the angular distribution is dependent on the dilepton mass $m_{\ell\ell}$ spectrum and polarization measurements based on this spectrum are sensitive to new physics.

$$V_{td} \sim \lambda^3(1 - \rho - i\eta) \tag{4}$$

The decay topology is contructed by looking for the well displaced tericary K^0_S vertex, recontructed through the $\pi^+\pi^-$decay mode, which then is used to fully recontruct the K^0_S momentum and point it back to a tight DCA with a B_s vertex defined by the muon tracks. The combination of the K^0_S reconstruction requirements, and the contraints placed on the B_s vertex in invarient mass and pt^2 make the mode free of most physics and combinatoric backgrounds. This is demonstrated with the reconstruction of the K^0_S with the BANA package for the P17 dataset as shown in figure 6. The combinatorial backgound under the K^0_S peak can be almost entirely eliminated by making an additional cut on the pt of the presumed pion tracks relative to the displacement between the K^0_S and a given secondary vertex.

There are currently no observation or limit on the decay $B_s \to K^0_S\mu^+\mu^-$.

2.2.2 $B_s \to \phi\mu^+\mu^-$

Similar to the $B_s \to K^0_S\mu^+\mu^-$ mode, the decay mode $B_s \to \phi\mu^+\mu^-$ is an associated decay that directly accesses the $b \to s$ penguin diagrams of figure 7.

The decay measures the strength of the couplings of $V_{tb}V^*_{ts}$ in the same manner as the direct dilepton $B_s \to \mu^+\mu^-$ mode. Measurement of $B_s \to \phi\mu^+\mu^-$ is an alternate method of accessing the Wolfenstien parameters. The decay topology though places addtional contrains on the final state which help to suppress backgrounds.

The final state most readily accessible is the $B_s \to \phi\mu^+\mu^- \to K^+K^-\mu^+\mu^-$. This places an invarient mass constraint on the kaon pair for a $\phi(1020)$ reconstruction and also provides a distinct four track displaced vertex. This mode is almost idential to the reconstruction used to detect the B_s through the $B_s \to J/\Psi\phi$

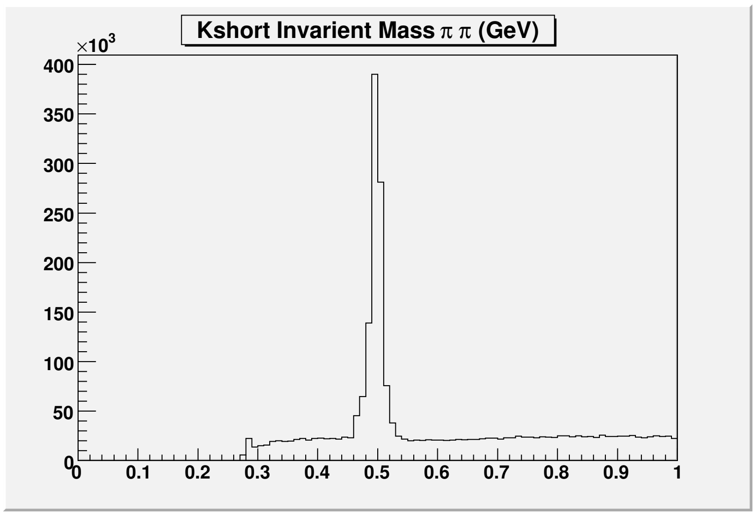

Figure 6: K_S^0 invarent mass reconstruction from the P17 dataset prior to pt_{rel} cut.

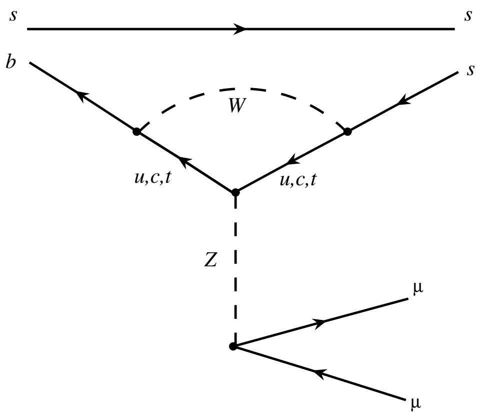

(a) $B_s \to \phi\mu^+\mu^-$ penguin 1

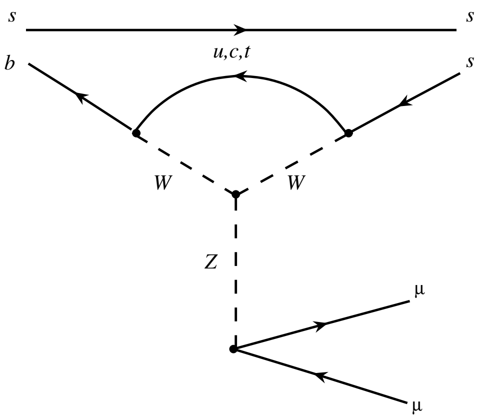

(b) $B_s \to \phi\mu^+\mu^-$ penguin 2

Figure 7: Associated decay $B_s \to \phi\mu^+\mu^-$.

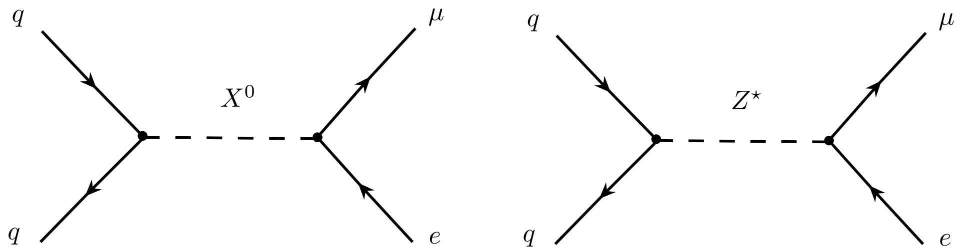

(a) Direct LFV coupling to X^0 (b) Direct LFV coupling to an excited heavy Z^*

Figure 8: Direct charged lepton flavor violation via beyond standard model couplings

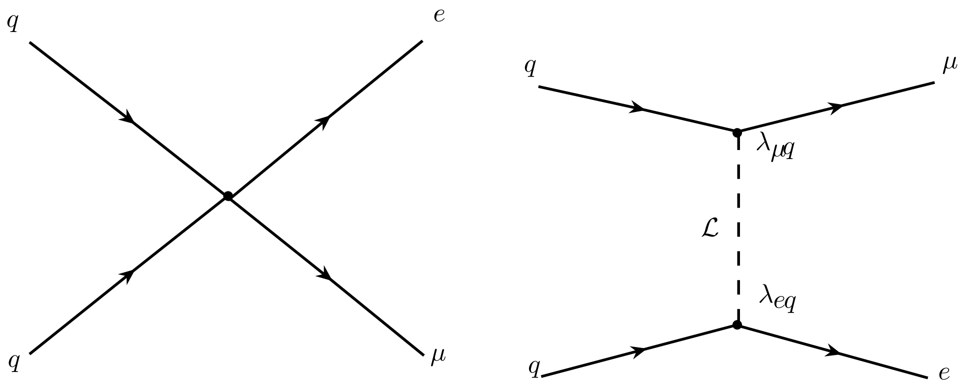

(a) Direct LFV via a 4-fermion point interaction (b) Direct LFV through a lepto-quark interaction

Figure 9: Direct charged lepton flavor violation in 4-fermion and leptoquark

channel, where the J/Ψ is force through the $\mu^+\mu^-$ channel and the ϕ through the kaon pair. This then also allows a natural normalization of the decay directly to the $J/\Psi\phi$ channel as the majority of systemmatics and acceptances will cancel in the branching fraction ratio.

Currently the decay $B_s \rightarrow \phi\mu^+\mu^-$ has not been observed, with a limit on the branching fraction of 3.2×10^{-6}.

3 Lepton Flavor Violation (LFV)

The subject of lepton flavor violation has received considerable interest since the observation that the neutrino species are massive and exhibit almost maximal mixing between $\nu_2 \rightarrow \neq_3$. This mixing in the neutral leptons is a non-standard model effect and as such leads to the natural question of whether the charged leptons also have non-zero mixing between generations. In this case the search is for a process that can mix $\mu \rightarrow e$, $\tau \rightarrow \mu$ or $\tau \rightarrow e$.

These mixing can occur in a number of different fashions, ranging from direct cross flavor couplings to new heavy neutral current (a new particle X^0, or an excited Z^* type state) as shown in figure 8

Additional possibilities for LFV include four-fermion point interaction vertices's or lepto-quark type couplings as shown in figure 9

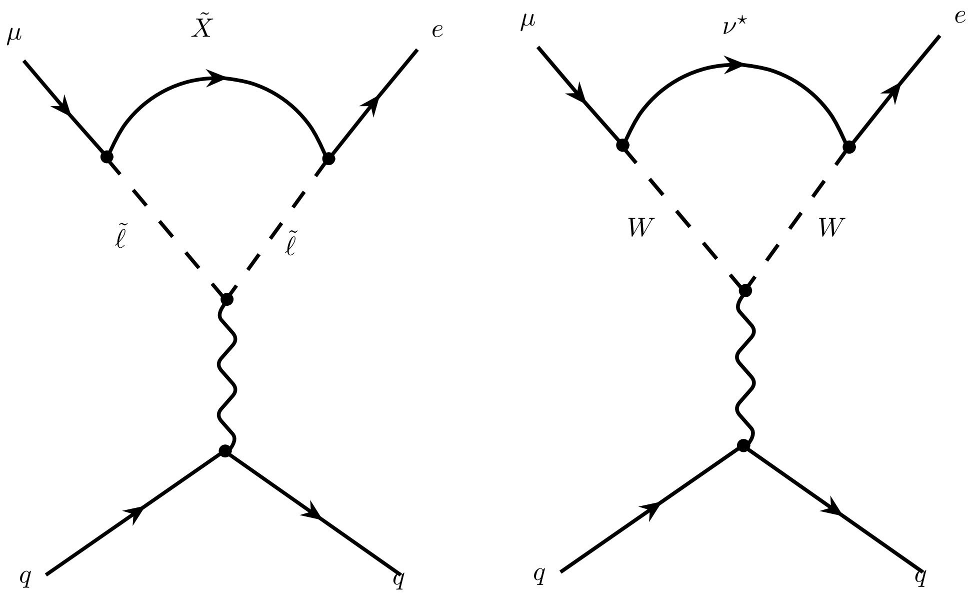

(a) Indirect LFV through a SUSY loop (b) Indirect LFV through a heavy ν loop

Figure 10: Indirect charged lepton flavor violating processes

Indirect LFV can occur in many extensions to the standard model and include SUSY penguins and heavy neutrino loops. These couplings are shown in figure 10

The B-meson sector is an ideal system for examining these types of possible couples. In each case the $q\bar{q}$ state serves as the natural hook for the process with the high mass of the b-quark serving to help boost the decay rate compared to the equivalent processes in the light meson sectors.

In what follows we examine the class of decays with a μe final state lepton signature, although in most cases the analogous modes that include a τ can be examined with good enough τ identification.

3.0.3 Two body $B_s \to \mu^{\pm} e^{\mp}$ and $B^0 \to \mu^{\pm} e^{\mp}$

The two body final states of $B_s \to \mu^{\pm} e^{\mp}$ and $B^0 \to \mu^{\pm} e^{\mp}$ provide the base measurement for exploring charged lepton flavor violation. In each of these decays modes we can search for simply the di-lepton final state, reconstructed to a displaced B-vertex with definite invariant mass and low pt^2 to the primary.

The primary backgrounds for these processes are the misidentification of overlap between semileptonic b decays where the secondary vertex resolution is insufficient to distinguish between the separate decays, and from overlap with the leptons from prompt W's. The use of vertex significance cuts and lepton momentum asymmetry cuts should reduces these types of backgrounds significantly, but require detailed studies to determine the amount of background rejection they can achieve.

Currently the limits on the observation of $B_s \to \mu^{\pm} e^{\mp}$ are shown in table 2.

From the table we can see that the current limit for $B_s \to \mu^{\pm} e^{\mp}$ is well within the sensitivity of the $D\O$data sets, while the B^0 mode may be near the current limit depending on the intrinsic backgrounds at that level.

Decay	Limit	Source
$B_s \to \mu^{\pm}e^{\mp}$	6.1×10^{-6}	CDF PRL 81 5742
$B^0 \to \mu^{\pm}e^{\mp}$	9.2×10^{-8}	BABAR PR D77 032007

Table 2: Current limits on $\mu^{\pm}e^{\mp}$type B_s and B^0 decays.

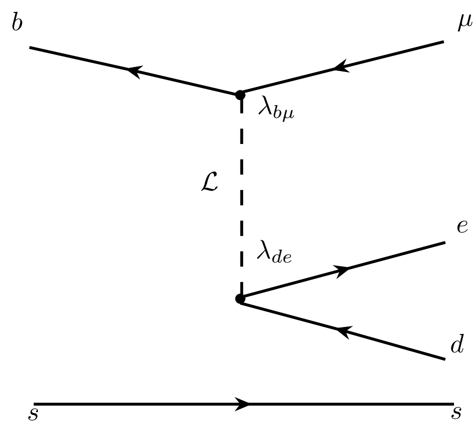

Figure 11: The decay $B_s \to K^0_S\mu^{\pm}e^{\mp}$ proceeding through a lepto-quark style interaction where the amplitude becomes proportional to the couplings $\lambda_{b\mu}$ and λ_{de}. The standard GIM suppression of the FCNC does not not apply in this case allowing larger than expected amplitudes compared to the standard model $B_s \to K^0_S\mu^+\mu^-$ channel.

3.0.4 Associated CLFV $\mu^{\pm}e^{\mp}$modes

In the same manner as the associated dileptonic mode variation of the $B_s \to \mu^+\mu^-$ channel can yield valuable information to the CKM mixing, the associated decay mode variations to $B_s \to \mu^{\pm}e^{\mp}$ provide addtional channels to search for non-standard model effects.

In the case of the neutral mesons it is interesting to examine the channels $B_s \to K^0_S\mu^{\pm}e^{\mp}$ and $B_s \to \phi\mu^{\pm}e^{\mp}$. In each of these decays the $b \to s$ or $b \to d$ transition that is normally GIM suppressed, need not have its amplitude highly reduced if the process couples to a tree level lepton flavor violating process or to a lepto-quark or 4-fermion vertex type interaction. In these cases the amplitude processed relative to the strength of the coupling of the LFV process and the observed amplitude then provides model constrains. This effect is shown in figure 11 for the $B_s \to K^0_S\mu^{\pm}e^{\mp}$ mode.

The other mode that exhibits this type of effect is the decay $B_s \to \phi\mu^{\pm}e^{\mp}$ where again the $b \to s$ transition need no longer occur at loop level, but can proceed via a tree level diagram that accesses one of the non-standard model propagators. In this case the process probes the second generation quark/lepton couplings and in combination with the $B_s \to K^0_S\mu^{\pm}e^{\mp}$ mode allows extraction of the third generation couplings.

From an experimental point of view these modes are favorable due to the clean final state signature they they pose. Similar to their stand model dileptonic counter parts the well defined K^0_S signature with reconstruct back to a secondary b-vertex, or the four track secondary K^+K^- $\mu^{\pm}e^{\mp}$with the $\phi(1020)$ constraint, provide clean signatures that are difficult to mimic with other physics processes.

Currently there are no limits on the observation of either of these modes, although the corresponding charm analogs ($D^0 \to K^0_S\mu^{\pm}e^{\mp}$) have been searched for. This makes the search for LFV in the associated channels especially interesting.

The associated channels can also be searched for in the charged B sector, where the decays of interest

Decay	Limit	Notes
$B_s \to K_S^0 \mu^\pm e^\mp$	none	
$B_s \to \phi \mu^\pm e^\mp$	none	
$B^+ \to K^+ \mu^\pm e^\mp$	6×10^{-3}, 8×10^{-7}	$\mu^+ e^-$ vs. $\mu^- e^+$
$B^+ \to \pi^+ \mu^\pm e^\mp$	6×10^{-3}	

Table 3: Current limits on $\mu^\pm e^\mp$type associated channel B meson decays.

Final state	Limit	Notes
$\pi^+\pi^-$	1.7×10^{-6}	CP
$\phi\phi$	observed: 1.4×10^{-5}	polarization
K^+K^-	observed: 3.3×10^{-5}	polarization
π^+K^-	5.6×10^{-6}	CP
ϕK^*	1.0×10^{-3}	polarization
pp	5.9×10^{-5}	

Table 4: Two body final states B_s decays with sensitivity to new physics or CP violation.

become $B^+ \to K^+ \mu^\pm e^\mp$ and $B^+ \to \pi^+ \mu^\pm e^\mp$. The current limits for these decays are listed in table 3

4 CP Violation ($/CP$)

CP violation in the B sector is most notable in the direct measurement of B_s mixing. There are however other decays that can measure the degree of CP violation in the sector through the final state couplings and polarizations of the decay daughters. In the context of the B_s system these fall primarily into the two meson final states where polarization or CP asymmetry gives a probe into non-standard model processes. Decays falling into this class which are detectable in the $D\O$data sets are listed in table 4 and while not an exhaustive list represent the more interesting decays that are available.